Nat Neurosci. Author manuscript; available in PMC 2016 September 15.

Published in final edited form as:

Nat Neurosci. 2014 April ; 17(4): 522–532. doi:10.1038/nn.3657.

Palmitoylation of δ-catenin by DHHC5 Mediates Activity-Induced Synapse Plasticity

G. Stefano Brigidi[1], **Yu Sun**[1], **Dayne Beccano-Kelly**[2], **Kimberley Pitman**[3], **Mahsan Mobasser**[1], **Stephanie L. Borgland**[3], **Austen J. Milnerwood**[2,4], and **Shernaz X. Bamji**[1]

[1]Department of Cellular & Physiological Sciences & the Brain Research Centre, University of British Columbia, 2350 Health Sciences Mall, Vancouver, B.C., V6T-1Z3, Canada

[2]Centre for Applied Neurogenetics, Department of Medical Genetics & the Brain Research Centre, University of British Columbia, 2211 Wesbrook Mall, Vancouver, B.C., V6T-1Z3, Canada

[3]Department of Anesthesiology, Pharmacology & Therapeutics & the Brain Research Centre, University of British Columbia, 212-2176 Health Sciences Mall, Vancouver, B.C., V6T-1Z3, Canada

[4]Division of Neurology, Department of Medicine, University of British Columbia, 2211 Wesbrook Mall, Vancouver, B.C., V6T-1Z3, Canada

Abstract

Synaptic cadherin adhesion complexes are known to be key regulators of synapse plasticity. However, the molecular mechanisms that coordinate activity-induced modifications in cadherin localization and adhesion and subsequent changes in synapse morphology and efficacy, remain unanswered. We demonstrate that the intracellular cadherin binding protein, δ-catenin, is transiently palmitoylated by DHHC5 following enhanced synaptic activity, and that palmitoylation increases δ-catenin/cadherin interactions at synapses. Both the palmitoylation of δ-catenin and its binding to cadherin are required for activity-induced stabilization of N-cadherin at synapses, the enlargement of postsynaptic spines, as well as insertion of GluA1 and GluA2 subunits into the synaptic membrane and the concomitant increase in mEPSC amplitude. Importantly, context-dependent fear conditioning in mice results in increased δ-catenin palmitoylation as well as increased δ-catenin/cadherin associations at hippocampal synapses. Together, this suggests a role for palmitoylated δ-catenin in coordinating activity-dependent changes in synaptic adhesion molecules, synapse structure, and receptor localization that are involved in memory formation.

Address for correspondence: Shernaz X. Bamji, Ph.D., Department of Cellular & Physiological Sciences, University of British Columbia, 2350 Health Sciences Mall, Vancouver, B.C., V6T-1Z3, Canada, Tel: 604-822-4746, shernaz.bamji@ubc.ca.

Author Contributions: G.S.B. designed the project, conducted biochemistry, imaging, and behavioral experiments, and conducted data analysis. Y.S. generated mutant cDNA constructs, conducted biochemistry and imaging experiments, and data analysis. D.B.-K. and K.P. conducted electrophysiology experiments. D.B.-K., S.L.B., and A.J.M. designed electrophysiology experiments and conducted data analysis. M.M. conducted imaging experiments and data analysis. S.X.B. designed and supervised the project. G.S.B. and S.X.B. wrote the paper.

Keywords

δ-catenin; palmitoylation; cadherin; synapse; activity; hippocampal culture; protein trafficking; contextual fear conditioning

INTRODUCTION

Synaptic adhesion molecules, and in particular the classic cadherins, have been well studied with respect to their regulation of synapse function. Indeed, cadherins have been shown to be essential for activity-dependent structural remodeling, including enlargement of spines[1, 2] and increases in synapse number[3]. Activation of NMDA receptors enhances the clustering and stabilization of cadherins at synapses[4], and it is believed that this is essential for the establishment and maintenance of long-term potentiation (LTP)[1, 5] as well as the formation of long-term contextual memory[6].

The stability and clustering of cadherin at the cell membrane is primarily dictated by its interaction with intracellular catenins. Whereas cadherin/β-catenin interactions mediate intercellular cadherin interactions, cadherin *cis*-clustering is regulated by δ-catenin, p120-catenin (p120ctn), p0071, and ARVCF, that bind to the cadherin juxtamembrane domain[7]. δ-catenin is highly expressed in the brain, and is specifically enriched in dendritic spines, where it can link cadherin to the actin cytoskeleton[8], as well as to several postsynaptic scaffold molecules, including PSD-95[9] and GRIP[10]. The importance of δ-catenin in cognitive function and neural connectivity is supported by deficits in learning and memory, as well as synapse plasticity and morphology in δ-catenin-mutant mice[11–13]. Importantly, mutations of δ-catenin have been associated with severe impairments of cognitive function[14], and may underlie the mental disabilities associated with *Cri-du-Chat* syndrome and schizophrenia[15, 16].

δ-catenin has been identified as a substrate for protein palmitoylation[17], a reversible post-translational modification involving the addition of palmitate to cysteine residues, mediated by a family of palmitoyl-acyl transferase (PAT) enzymes containing a conserved Asp-His-His-Cys (DHHC) motif[18]. Recent work has demonstrated that palmitoylation of synaptic proteins can be enhanced following neuronal activity[19, 20], and can increase the trafficking of these proteins to the synapse[19, 20].

Previous work *in vitro* clearly point to a role for cadherins in activity-mediated synapse plasticity. However, the molecular mechanisms that translate enhanced neuronal activity to changes in cadherin-based adhesion and synaptic remodeling remain poorly understood. Here we demonstrate that the dynamic palmitoylation of δ-catenin by DHHC5 can coordinate activity-dependent changes in synapse adhesion, structure, and the efficacy of synaptic transmission. Together, this suggests a key role for δ-catenin in what are widely regarded as fundamental molecular processes underlying learning and memory.

RESULTS

Activity-dependent palmitoylation of δ-catenin in neurons

We determined whether palmitoylation of δ-catenin is regulated by activity using the acyl-biotin exchange (ABE) assay, which exchanges palmitoyl modifications with biotin[18, 20, 21]. Hydroxylamine (NH_2OH) is essential for the biotinylation of cysteine residues as it cleaves palmitate from cysteine residues. Exclusion of hydroxylamine is therefore used as a control for the specificity of biotin labeling[22].

15–16 days *in vitro* (DIV) hippocampal neurons were treated with a glycine/bicuculline solution for 3 minutes. This method has previously been used to induce LTP in hippocampal slices[23], and enhance structural remodeling of excitatory synapses in cultured neurons by activating synaptic NMDA receptors[24, 25], and will hereafter be referred to as chemical LTP (cLTP). δ-catenin palmitoylation was significantly enhanced 40 min following cLTP stimulation and was blocked by D-AP5 (50μM), demonstrating the involvement of NMDA receptors (Fig. 1a, b). We next examined the time-course of activity-induced δ-catenin palmitoylation and compared it to another palmitoylated synaptic protein, PSD-95[19]. δ-catenin palmitoylation significantly increased 20 min following cLTP, peaked at 40 min, and returned to basal levels by 180 min (Fig. 1c, d). In contrast, PSD-95 palmitoylation was maintained up to 180 min (Fig. S1a, b), indicating that PSD-95 is more stably palmitoylated, as previously suggested[21]. Thus, palmitoylation of δ-catenin is transiently increased following synaptic activation, and represents a distinct cellular event relative to another palmitoylated synaptic protein, PSD-95.

Long-term, homeostatic scaling of neuronal networks has been shown to regulate the palmitoylation of several synaptic proteins[26]. To examine if palmitoylation of δ-catenin is similarly modulated at a network level, hippocampal neurons were treated for 48 hours with tetrodotoxin (TTX; 1μM) to enhance synaptic network strength (Fig. S1e, f). δ-catenin palmitoylation increased 48 hours following TTX treatment in agreement with our observation that activity enhances δ-catenin palmitoylation.

Palmitoylation of δ-catenin regulates its binding to N-cadherin

As palmitoylation increases protein hydrophobicity and trafficking to the membrane[19, 21], we examined the effects of activity on the subcellular distribution of δ-catenin. Prior to stimulation, GFP-δ-catenin was diffusely distributed along dendrites (Fig. S2a). However, 40 minutes after cLTP, GFP-δ-catenin became increasingly clustered, as evidenced by a decrease in the area of δ-catenin puncta (Fig. 1e, and S2a) with a concomitant increase in fluorescence intensity (Fig. S2b). This was abolished in cells treated with glycine plus D-AP5 (Fig. S2c, d). In contrast, no change was observed in the area or intensity of N-cadherin puncta (Fig. 1e, and S2a–d). The colocalization of δ-catenin and N-cadherin also significantly increased 20–180 min after cLTP (Fig. 1f, and S2a). *Post hoc* immunostaining demonstrated an increased colocalization of N-cadherin/δ-catenin clusters with PSD-95 indicating that activity enhances the recruitment of δ-catenin to synaptic cadherin (Fig. 1g, and S2e).

We next determined whether the time course for δ-catenin/N-cadherin interactions was similar to that of δ-catenin palmitoylation and δ-catenin/N-cadherin colocalization. The association of δ-catenin with N-cadherin was increased 20 min after stimulation and maintained up to 180 min (Fig. S2g–j), in sharp contrast to the time course of δ-catenin palmitoylation, which decreased to basal levels 180 min after stimulation.

These results suggested that a transient increase in δ-catenin palmitoylation is required for activity-dependent recruitment of δ-catenin to cadherin clusters, but is not essential to maintain this interaction. To test this, we examined the association of δ-catenin and N-cadherin in the presence of the global palmitoylation blocker, 2-bromopalmitate (2BP; 50μM). When cells were treated with 2BP 0–40 min following cLTP, the activity-induced increase in δ-catenin/N-cadherin interactions was abolished (Fig. 1h, i). However, when cells were treated with 2BP from 40–180 min after cLTP treatment (a time frame during which δ-catenin is highly palmitoylated), the activity-induced increase in δ-catenin/N-cadherin interactions was maintained (Fig. 1h, i). This demonstrates that δ-catenin palmitoylation is not required for maintaining its interaction with N-cadherin.

To determine whether activity enhances the recruitment of δ-catenin specifically to surface cadherin, we isolated surface proteins through biotinylation and immunoprecipitation with Sulfo-NHS-SS-biotin at various time points and observed an activity-dependent increase in δ-catenin co-immunoprecipitated with the surface fraction (Fig. S2h, l). In contrast, there was no significant increase in the recruitment of p120ctn to the surface fraction (Fig. S2h, l). Together, these data demonstrate that activity-induced palmitoylation of δ-catenin increases its recruitment to surface N-cadherin at postsynaptic membranes, but that this association can be maintained in the absence of δ-catenin palmitoylation.

Identification of palmitoylated δ-catenin residues

To determine the role of palmitoylated δ-catenin at the synapse, we sought to generate palmitoylation-defective mutants of δ-catenin, which required identifying the palmitoylated cysteine residue(s). δ-catenin mutants in which cysteines were mutated to serines were generated and assayed for palmitoylation in HEK293T cells (Fig. 2a). δ-catenin palmitoylation was abolished when all 18 cysteines were mutated to serines (18CS) and when the 7 C-terminal cysteines were mutated to serines (CTD7CS), but not when the 11 N-terminal cysteines were mutated to serines (NTD11CS), suggesting that one or more of the 7 C-terminal cysteine residues are the sites for palmitoylation (Fig. 2a–c).

We next mutated each of the 7 C-terminal cysteine residues to serines (GFP-δ-catenin C791S, C804S, C827S, and C853S, C906S, C960-1S), and assayed their palmitoylation compared to WT and CTD7CS δ-catenin. Point mutants C791S, C804S, C827S, C853S, and C906S were palmitoylated as robustly as WT, whereas palmitoylation of C960-1S was significantly reduced compared to WT (Fig. 2b, c). This strongly suggested that cysteines 960 and 961, which are also highly predicted to be palmitoylated (CSS-Palm 3.0,[27]), are the sites of palmitoylation. To verify this we generated a δ-catenin mutant in which all cysteines, with the exception of cysteines 960 and 961, were mutated to serines (NTD16CS). Palmitoylation of NTD16CS was similar to that of WT, demonstrating that cysteines 960 and 961 are necessary and sufficient for the palmitoylation of δ-catenin (Fig. 2b, c).

Identification of δ-catenin residues required for cadherin-binding

To determine whether palmitoylation of δ-catenin has a role beyond its regulation of δ-catenin/cadherin interactions, we sought to generate a δ-catenin mutant that could not bind to cadherin. Lysine residue 401 on p120ctn is required for p120ctn's association with cadherin[28] and the corresponding lysine on δ-catenin (lysine 581) was mutated to methionine (GFP-δ-catenin K581M). Immunoprecipitation assays in 293T cells demonstrated minimal association between δ-catenin K581M and N-cadherin compared to WT δ-catenin (Fig. 2d, e). Although the palmitoylation-deficient C960-1S mutant exhibited a significant reduction in its ability to bind cadherin compared to WT δ-catenin, it still exhibited significantly more binding compared to the K581M mutant (Fig. 2d, e). The addition of palmitate to δ-catenin therefore functions to target δ-catenin to the membrane where it associates with N-cadherin, but is not absolutely required for binding. Finally, we also generated short hairpin RNAs against δ-catenin (shRNA) and a control mismatch (shRNA-c) using previously described target sequences[29] and validated them in 293T cells (Fig. 2f, g).

Palmitoylated δ-catenin stabilizes N-cadherin at synapses

We next determined the role of δ-catenin palmitoylation in regulating cadherin stability within postsynaptic spine heads using fluorescence recovery after photobleaching (FRAP). Hippocampal neurons were transfected at 10 DIV with N-cadherin-RFP, δ-catenin shRNA, and shRNA-resistant (*) δ-catenin WT, K581M, or C960-1S constructs. FRAP assays were done 5–6 days after transfection, as previously reported to ensure knockdown of endogenous δ-catenin[29]. Cells were imaged 40–60 minutes after cLTP, or control buffer lacking glycine. We observed no differences in the initial fluorescence intensity of N-cadherin clusters in all groups analyzed (Fig. S3a).

N-cadherin-RFP clusters within dendritic spines were identified and a region of interest (ROI) of 1μm diameter was photobleached using a 405nm laser. The fluorescence recovery of N-cadherin-RFP within the photobleached ROI was determined over 5 min of time-lapse imaging, and normalized to a control ROI in an adjacent spine (Fig. 3a, b). In control neurons expressing GFP and shRNA-c, the fluorescence recovery of N-cadherin-RFP plateaued at 50.6 ± 8.0% (mean ± SEM) 5 mins after photobleaching (Fig. 4a, c, i), consistent with previous reports[31, 32]. Activity has been shown to stabilize N-cadherin at the synapse[4] and accordingly, glycine treatment dramatically reduced the fluorescence recovery of N-cadherin-RFP to 14.9 ± 7.4%. Treatment with glycine plus D-AP5 (50μM) abolished activity-induced stabilization of cadherin, resulting in fluorescence recovery similar to that of untreated cells (53.6 ± 4.8%; Fig. 3a, c, i).

Overexpression of WT δ-catenin increased the stability of N-cadherin under basal conditions and occluded further activity-dependent stabilization of N-cadherin (Fig. 3d, i). In contrast, overexpression of K581M and C960-1S did not impact the stability of N-cadherin under basal conditions suggesting that δ-catenin's palmitoylation and binding to cadherin are required for N-cadherin stabilization (Fig. S3b, c). Acute knockdown of δ-catenin using shRNA substantially decreased cadherin stability under basal conditions and abolished activity-dependent stabilization of N-cadherin (Fig. 3e, i). Introducing shRNA-resistant δ-

catenin (WT*) to shRNA-expressing cells rescued the shRNA phenotype, demonstrating that this was not due to off-target effects (Fig. 3f, i). Our data showing a requirement for δ-catenin for the stabilization of N-cadherin at synapses is in accord with previous work showing that ablation of δ-catenin reduces N-cadherin at the synapse[11, 13, 30].

To examine whether δ-catenin binding to cadherin is essential for activity-induced cadherin stabilization, we knocked down δ-catenin and expressed the cadherin-binding mutant, K581M*. Similarly, to examine whether palmitoylation of δ-catenin is important for activity-induced cadherin stabilization, we knocked down δ-catenin and expressed the palmitoylation mutant, C960-1S* GFP-δ-catenin. Abolishing δ-catenin's association with cadherin (Fig. 3g, i) or δ-catenin palmitoylation (Fig. 3h, i) significantly reduced the stability of N-cadherin under basal conditions and abolished activity-dependent stabilization of N-cadherin (Fig. 3g, h, i). Together, this demonstrates that the palmitoylation of δ-catenin, and its binding to cadherin are required for the stabilization of N-cadherin at synapses both under basal conditions and following enhanced neuronal activity.

Palmitoylated δ-catenin regulates activity-dependent spine remodeling

As palmitoylated δ-catenin stabilizes N-cadherin within spines, we next investigated if it is important for activity-dependent spine remodeling. 10 DIV neurons were transfected with GFP, shRNAs, and the indicated δ-catenin constructs. 5–6 days later, all spiny protrusions were imaged before and 40–60 minutes after cLTP. Neurons expressing GFP and shRNA-c exhibited spine head width, length, and density consistent with previous descriptions of spine morphology[28, 32] (Fig. 4a, g–i). cLTP treatment dramatically enhanced the width and density of protrusions and overexpression of δ-catenin increased the overall length and total density of protrusions (Fig. 4a, g, i), consistent with previous reports[25, 33,13, 34]. We also observed an increase in protrusion head width and the density of mature spines, with a reduction in filopodia density compared to control cells (Fig. 4b, g–i). None of these parameters were changed following cLTP.

Knockdown of δ-catenin resulted in protrusions with a filopodial appearance, including a decrease in protrusion width, an increase in protrusion length and an overall increase in the proportion of filopodia compared to spines, consistent with previous reports[8, 13]. Notably, cLTP did not alter any of these parameters (Fig. 4c, g–i). WT* δ-catenin rescued the phenotype observed in shRNA expressing cells, demonstrating that these morphological changes were not the result of off-target effects (Fig. 4d, g, h). Rescue with WT* δ-catenin also increased basal spine density consistent with that observed following δ-catenin overexpression. Expression of K581M* (Fig. 4e) or C960-1S* (Fig. 4f) in a δ-catenin knockdown background resulted in a phenotype similar to that of δ-catenin knockdown (Fig. 4c), with the exception of spine/protrusion density, which was similar to control (Fig. 4i). δ-catenin knockdown has been shown to increase the density of spiny protrusions via the PDZ binding motif of δ-catenin, and not through cadherin binding[13], corroborating well with our data. Notably, cLTP failed to alter protrusion morphology or density (Fig. 4e, f, g–i). Together, this demonstrates that palmitoylation of δ-catenin and its binding to cadherin are required for activity-dependent changes in spine morphology, but not density.

Palmitoylated δ-catenin is required for activity-induced synapse function

δ-catenin can associate with several postsynaptic scaffold molecules and AMPA receptor (AMPAR) binding proteins in a PDZ-dependent manner[9, 10, 35]. We therefore hypothesized that activity-induced palmitoylation of δ-catenin and the subsequent surface stabilization of cadherin in spine heads may be important for the insertion and stabilization of AMPARs at pre-existing synapses. To visualize surface AMPARs, GluA1 or GluA2 subunits were tagged with super-ecliptic pHluorin (SEP-GluA1, or SEP-GluA2, respectively). Neurons were transfected at 10 DIV with SEP-GluA1 or SEP-GluA2, shRNAs, and either RFP or the indicated RFP-δ-catenin constructs, and imaged before and after cLTP at 15–16 DIV. Clusters of SEP-GluA1 (Fig. S4a) and GluA2 (not shown) localized to spine heads under basal conditions in neurons expressing shRNA-c plus RFP. Under basal conditions the integrated density (IntDen; product of mean grey value and area) of GluA1surface clusters were similar for all conditions examined ($p=0.082$, $F_{5,71}=2.492$; one-way ANOVA) (Fig. S4a). The IntDen of GluA2 surface clusters was increased in δ-catenin overexpressing cells compared to control (1.48 ± 0.13 fold; $p<0.05$), in agreement with our observation of enlarged spine heads among these cells (Fig. 4b, g, h), but was similar among all other groups ($p=0.039$, $F_{5,69}=2.053$; one-way ANOVA).

40–60 min after cLTP there was a significant increase in the IntDen of GluA1 (Fig. 5a, and S4a) and GluA2 clusters in shRNA-c cells (Fig. S4b), compared to the same clusters before activity, consistent with previous reports[36, 37]. This was abolished in the presence of D-AP5 (50μM; Fig. 5a, and S4b). Interestingly, both overexpression and knockdown of δ-catenin abolished activity-induced insertion of GluA1 and GluA2 into the synaptic membrane (Fig. 5a, and S4a, b). WT* δ-catenin, but not the K581M* and C960-1S* δ-catenin mutants, rescued the shRNA phenotype (Fig. 6b, c), indicating that δ-catenin palmitoylation and binding to cadherin are essential for activity-induced insertion of AMPARs into the synaptic membrane.

δ-catenin overexpression (shRNAc + WT) enhanced the colocalization of δ-catenin and SEP-tagged GluA1 and GluA2 subunits under basal conditions compared to cells expressing shRNA + WT* (wildtype rescue, control) (Fig. 5b, and S4c). This suggests that overexpressing δ-catenin increases its localization at synapses and accounts for the observed increase in surface GluA2 levels under basal conditions. In contrast, the localization of the cadherin-binding mutant (shRNA + K581M*) at synapses was significantly decreased but not abolished (Fig. 5b, and S4c), indicating that other motifs including its PDZ-binding domain may also be involved. The δ-catenin palmitoylation mutant (shRNA + C960-1S*) exhibited similar synaptic localization as controls (shRNA + δ-catenin WT*). Since this mutation does not abolish binding to cadherin entirely, the C960-1S mutant may localize to synapses through cadherin interactions as well as through other binding motifs including its PDZ-binding domain.

Following cLTP, we observed an increase in the recruitment of δ-catenin to synapses in control (shRNA + WT*) and δ-catenin overexpressing (shRNA-c + WT) cells (Fig. 5b, and S4c). In contrast, cLTP did not increase the recruitment of cadherin-binding deficient or palmitoylation-deficient δ-catenin to synapses.

To confirm that δ-catenin does not overall impact overall exocytosis, we examined turnover of the transferrin receptor tagged with SEP and mCherry (TfR-mCherry-SEP)[37]. Activity enhanced TfR-mCherry-SEP florescence in control cells, as well as cells overexpressing δ-catenin, and knockdown cells (Fig. S4d), demonstrating that δ-catenin plays a specific role in regulating the surface insertion and stabilization of AMPAR cargo, and not overall cellular exocytosis or trafficking.

We next determined whether δ-catenin palmitoylation is required for glycine-mediated enhancement of miniature excitatory post-synaptic currents (mEPSCs)[24, 25]. Neurons were transfected at 10 DIV with the indicated shRNAs and GFP or GFP-tagged δ-catenin constructs. 5 days later, we obtained whole-cell voltage clamp recordings 40 min after cLTP. Under basal conditions, we observed increased mEPSC amplitude and frequency in δ-catenin overexpressing cells relative to control (Fig. 5c–e), consistent with our observation of increased spine density (Fig. 4i) and surface GluA2-AMPARs in these cells[35]. There were no significant differences in basal mEPSC amplitude and frequency between any of the other groups relative to control cells (Fig. 5c–e). cLTP significantly increased the amplitude and frequency of mEPSCs in cells expressing shRNA-c (Fig. 5c, f, g). Overexpression and knockdown of δ-catenin abolished this effect, which was restored in knockdown neurons expressing δ-catenin WT* (Fig. 5c, f, g). Notably, expression of palmitoylation-deficient δ-catenin C960-1S* did not rescue the glycine-induced increase in mEPSC amplitude and frequency (Fig. 5c, f, g). These findings demonstrate that palmitoylated δ-catenin is required for activity-induced enhancement of mEPSC amplitude and frequency.

δ-catenin palmitoylation increases following acquisition of contextual fear memory

We next investigated whether palmitoylated δ-catenin is involved in learning and memory using a hippocampal-dependent, contextual fear-conditioning paradigm[6] (Fig. 6a). Conditioned mice exhibited enhanced freezing 1 h and 24 h after reintroduction to the context where they received a single foot shock (0.3mA, 5sec), demonstrating acquisition of contextual memory (Fig. 6a). Immediately following testing, mice were sacrificed and hippocampal and cortical tissue isolated for biochemical analyses. Palmitoylation of δ-catenin in the hippocampus was significantly increased 1 h after training, but returned to baseline 24 h after training (Fig. 6b, c), demonstrating transient palmitoylation similar that observed in hippocampal cultures following cLTP (Fig. 1c, d). In contrast, δ-catenin palmitoylation was unchanged in the cortex following fear conditioning (Fig. 6d, e), demonstrating specificity for δ-catenin palmitoylation in the hippocampus following the formation of contextual memories.

We next examined the effects of fear conditioning on δ-catenin/N-cadherin interactions at the synapse. There was a significant increase in δ-catenin/cadherin interactions in P2 synaptosomal fractions both 1 and 24 h after conditioning (Fig. 6f, g). This relatively stable increase in the association between δ-catenin and cadherin following fear conditioning was similar to that observed in cultured neurons following increased activity (Fig. S2i, j). Our findings are consistent with the interpretation that a transient increase in palmitoylation of δ-catenin targets it for a more stable association with N-cadherin at hippocampal synapses *in vivo*, and is correlated with the acquisition of contextual fear memories.

DHHC5 is required for activity-dependent palmitoylation of δ-catenin

We next sought to identify the DHHC protein that palmitoylates δ-catenin in an activity-dependent manner. Although 23 mammalian DHHC proteins have been identified[18], only 17 of these have been shown to have PAT activity[38]. We co-expressed each of these 17 DHHC proteins with δ-catenin in HEK293T cells and tested for δ-catenin palmitoylation (Fig. 7a, b). DHHC5 and DHHC20 significantly increased δ-catenin palmitoylation relative to a vector control, indicating that these proteins are sufficient for δ-catenin palmitoylation (Fig. 7a, b).

We performed a second overexpression screen in neurons using DHHC proteins that are expressed in the brain, and which have known synaptic protein substrates ([18], Allen Mouse Brain Atlas; http://mouse.brain-map.org/). Overexpression of DHHC5 and 20 enhanced δ-catenin/N-cadherin colocalization in the absence of cLTP (Fig. 7c, and S5a), and this enhanced clustering was abolished in cells expressing the δ-catenin C960-1S mutant (Fig. 7d, and S5b). Together, this indicates that DHHC5 and 20 are sufficient to enhance the recruitment of δ-catenin to cadherin clusters by palmitoylating δ-catenin in neurons.

We next determined whether DHHC5 and DHHC20 are necessary for activity-dependent palmitoylation of δ-catenin. The efficacy of DHHC5 shRNA (shRNA-D5;[21]) and DHHC20 siRNA (siRNA-D20) were first validated in neurons (Fig. 7e, f). Activity-induced recruitment of δ-catenin to N-cadherin clusters was abolished in neurons expressing shRNA-D5 but not siRNA-D20 (Fig. 7g). These results indicate that although both DHHC5 and 20 are *sufficient* to palmitoylate δ-catenin, only DHHC5 is *required* for activity-induced palmitoylation of δ-catenin and the activity-dependent targeting of δ-catenin to cadherin.

We assayed δ-catenin palmitoylation in DHHC5 knockdown cells to confirm our observations. We first confirmed that the DHHC5 knockdown observed at 6 DIV (Fig. 7e) persisted for up to 12 DIV (Fig. 8a). The knockdown in individual cells was robust, with a 40% decrease in DHHC5 levels reflecting the transfection efficiency of Amaxa nucleofection (approximately 50%). Basal levels of δ-catenin palmitoylation did not appear to be significantly reduced in cells expressing DHHC5 shRNA (Fig. 8a, b). However, activity-dependent increase in δ-catenin palmitoylation was abolished in these cells and restored in cells co-expressing shRNA-resistant DHHC5 (Fig. 8a, b). Together, this strongly indicates that DHHC5 is required for activity-dependent palmitoylation of δ-catenin.

DHHC5 has previously been shown to accelerate the constitutive delivery of AMPARs to the cell surface through palmitoylation of the δ-catenin binding partner, GRIP1b[10, 21]. However, it is unknown whether DHHC5 plays a role in activity-dependent recruitment of AMPARs to the cell surface. As expected, we observed a robust increase in the IntDen of SEP-GluA1 clusters 40 min after cLTP in control neurons (vector+ shRNA-c; Fig. 8c, d). Neurons overexpressing DHHC5 exhibited a significant increase in the basal IntDen of SEP-GluA1, consistent with a role for DHHC5 in constitutive AMPAR surface delivery[21], and also exhibited a further activity-dependent increase in AMPAR recruitment to the membrane (DHHC5+shRNA-c; Fig. 8c, d). We observed a similar basal increase in SEP-GluA1 IntDen in neurons expressing DHHC5 plus δ-catenin shRNA, in line with the observation that DHHC5 enhances the recruitment of AMPAR to the cell surface through palmitoylation of

another substrate. However, the activity-dependent increase in the IntDen of SEP-GluA1was abolished in these cells. Expression of shRNA-resistant δ-catenin (WT*) rescued the effect of knocking down δ-catenin in DHHC5 expressing cells, whereas expression of palmitoylation-defective δ-catenin (C960-1S*) did not (Fig. 8c, d). Together, this clearly demonstrates that DHHC5 mediates activity-induced insertion of AMPARs to the cell surface through palmitoylation of δ-catenin. The increase in the IntDen of SEP-GluA1 under basal conditions was maintained in δ-catenin knockdown cells, WT rescue cells, and C960-1S rescue cells (Fig. 8c, d), indicating that palmitoylation of δ-catenin by DHHC5 is not required for constitutive AMPAR surface delivery.

We also observed significantly more δ-catenin WT/GluA1 colocalization compared to δ-catenin C960-1S/GluA1 colocalization at basal levels in cells expressing DHHC5. Moreover, activity significantly enhanced δ-catenin WT/GluA1 colocalization, but had no effect on δ-catenin C960-1S/GluA1 colocalization (Fig. 8e).

DISCUSSION

Our study demonstrates that palmitoylated δ-catenin mediates changes in synapse adhesion, structure, and efficacy that are correlated with neuronal activity and the formation of new memories. We have demonstrated that enhanced synaptic activity results in a transient increase in the palmitoylation of δ-catenin, which targets it for a lasting association with N-cadherin at the postsynaptic membrane. Notably, we observed that the binding of δ-catenin to N-cadherin confers increased stability to cadherin molecules within spine heads and in turn, allows the activity-dependent remodeling of spines and the insertion of synaptic AMPARs. Consistently, the palmitoylation of δ-catenin is essential for activity-dependent increases in mEPSC amplitude and frequency. Moreover, we demonstrate that the acquisition of context-dependent fear memory is correlated with a transient increase in the palmitoylation of δ-catenin and a concomitant increase in synaptic cadherin/δ-catenin interactions specifically within the hippocampus. This temporal agreement between our *in vitro* and *in vivo* results underscore our model that palmitoylation of δ-catenin drives changes in the structure and efficacy of synapses believed to underlie learning and memory. Finally, we demonstrated that DHHC5 and DHHC20 are sufficient to palmitoylate δ-catenin, whereas only DHHC5 is required for activity-induced increase in δ-catenin palmitoylation. Intriguingly, we demonstrate that DHHC5 mediates activity-induced surface insertion of AMPARs through palmitoylation of δ-catenin.

The stability of N-cadherin at the membrane is known to be regulated by the catenins[7]. Binding of p120ctn to the cadherin juxtamembrane domain stabilizes surface cadherin by masking endocytic motifs[28, 39], and it is possible that δ-catenin stabilizes cadherin by the same mechanism. Indeed, δ-catenin associates with the identical region of the cadherin juxtamembrane domain as p120ctn and both utilize a conserved lysine residue to bind cadherin[28]. Although it is tempting to speculate that palmitoylation of δ-catenin provides a competitive advantage for binding to cadherin following increased activity, we have observed increased cadherin/δ-catenin interactions with no significant changes in cadherin/p120ctn interactions. Activity-dependent recruitment of β-catenin to synaptic cadherin has also been shown to stabilize cadherin within the membrane[4]. As β-catenin interacts with the

C-terminal domain of cadherin[40], a region distinct from the site of δ-catenin interaction, it likely that activity-driven post-translational modifications of both β-catenin and δ-catenin are important for regulating cadherin surface stability.

Cadherin clustering within spine heads has been shown to be essential for activity-induced spine remodeling in cultured neurons[2] and *in vivo*[1]. It is possible that the palmitoylation of δ-catenin and its binding to cadherin promote spine remodeling by increasing the interactions of membrane-bound cadherin with the actin cytoskeleton through its association with α-catenin[41]. It is also possible that δ-catenin regulates spine morphology more directly, through its interaction with actin-binding proteins, including cortactin[42] and several Rho-GTPases[8] (but see[34]). Notably, knockdown of δ-catenin enhances protrusion density through mechanisms involving its PDZ-binding domain and not by its ability to bind cadherin[13]. Consistent with this report, we show that spine density is not significantly changed in neurons expressing δ-catenin K581M or C960-1S. Together, our results suggest that δ-catenin palmitoylation and cadherin-binding are primarily important for spine remodeling and maturation, whereas a δ-catenin's interactions with actin-binding proteins and an unknown signaling mechanism via its PDZ domain can regulate protrusion density.

The reversible addition of palmitate to synaptic proteins can dramatically impact their trafficking and localization, however the regulation and temporal profile for synaptic protein palmitoylation varies greatly between substrates[19, 21]. For example, activity regulates the palmitoylation of PSD-95, resulting in a relatively stable modification of this protein[19, 21] (but see[43]). In contrast, palmitoylation of the synaptic adaptor protein, GRIP1b, is not activity-dependent and exhibits a strikingly high rate of palmitate turnover[21]. Thus, the transient activity-dependent increase in δ-catenin palmitoylation is distinctive and does not merely reflect generalized changes in synaptic protein palmitoylation.

It is interesting to speculate that δ-catenin may cooperate with GRIP1b to mediate surface insertion of AMPARs. Palmitoylation of δ-catenin by DHHC5 is specifically required for activity-dependent increases in surface AMPARs, whereas palmitoylation of GRIP1b by DHHC5 mediates constitutive delivery of AMPARs to the cell surface[21]. We hypothesize that constitutive palmitoylation of GRIP1b regulates the mobilization and delivery of AMPARs to synapses, whereas transient activity-dependent palmitoylation of δ-catenin increases the stable surface population of synaptic AMPARs.

There are two possible mechanisms by which δ-catenin palmitoylation and cadherin binding regulate surface AMPAR localization and synapse strength. First, δ-catenin localization at synapses may stabilize AMPARs at the synaptic surface by directly interacting with the scaffold molecules GRIP/ABP[10, 44] and PSD-95[9] through its PDZ binding motif. Second, δ-catenin may regulate the stability of AMPARs at the surface by stabilizing N-cadherin within the membrane and enhancing interactions between cadherin and AMPAR subunits. Indeed, N-cadherin has been shown to bind and stabilize GluA2 directly through its extracellular domain[32]. Moreover, GluA1-containing AMPARs have also been observed in complex with N-cadherin[45]. δ-catenin can therefore link N-cadherin with AMPARs both by interacting with adaptor proteins intracellularly, and by positioning more N-cadherin in the membrane and enabling the direct extracellular interaction between AMPARs and cadherin.

Our results suggest that loss of δ-catenin palmitoylation specifically disrupts activity-dependent plasticity, which is further supported by our demonstration of normal mEPSCs and surface AMPAR levels under basal conditions. However, it remains a possibility that perturbations in synapse plasticity are connected to subtle deficits in basal synapse function that result from loss of δ-catenin palmitoylation. More detailed experiments are required to determine whether more subtle changes in basal synapse function are impacting activity-induced plasticity.

Knockout studies have demonstrated a requirement for N-cadherin as well as δ-catenin and β-catenin in the formation of contextual memories[6, 11, 46]. Indeed, acute blockade of N-cadherin-mediated adhesion in the hippocampus *in vivo* inhibits contextual memory formation[6] and knockdown of β-catenin disrupts the consolidation of fear memories[46]. Interestingly, in stark contrast to what we observed for δ-catenin, fear conditioning resulted in a transient decrease in β-catenin/cadherin interactions associated with increased β-catenin phosphorylation[46]. It is likely that activity-driven post-translational modifications to both β-catenin and δ-catenin are important for regulating cadherin surface stability. However, the distinct time course for the association of cadherin with these catenins following learning suggests different roles for these molecules in memory acquisition and consolidation. Our data demonstrates that by increasing surface AMPARs and enhancing spine maturation and size, activity-driven palmitoylation of δ-catenin is a vital component for LTP and supports its involvement in learning and memory.

Supplementary Material

Refer to Web version on PubMed Central for supplementary material.

Acknowledgments

This work was supported by grants from Canadian Institutes of Health Research MOP-81158 (SXB), MOP-81144 (SXB), MOP-102617 (SLB) and MOP-119347 (AJM). Centre for Applied Neurogenetics is funded by the Canada Excellence Research Chair Program and the Leading Edge Endowment Fund. We are grateful to S. Jung, B. Jovellar, and B. Santyr for technical assistance on the project.

References

1. Bozdagi O, et al. Persistence of coordinated long-term potentiation and dendritic spine enlargement at mature hippocampal CA1 synapses requires N-cadherin. J Neurosci. 2010; 30:9984–9989. [PubMed: 20668183]
2. Mendez P, De Roo M, Poglia L, Klauser P, Muller D. N-cadherin mediates plasticity-induced long-term spine stabilization. J Cell Biol. 2010; 189:589–600. [PubMed: 20440002]
3. Bozdagi O, Shan W, Tanaka H, Benson DL, Huntley GW. Increasing numbers of synaptic puncta during late-phase LTP: N-cadherin is synthesized, recruited to synaptic sites, and required for potentiation. Neuron. 2000; 28:245–259. [PubMed: 11086998]
4. Tai CY, Mysore SP, Chiu C, Schuman EM. Activity-regulated N-cadherin endocytosis. Neuron. 2007; 54:771–785. [PubMed: 17553425]
5. Tang L, Hung CP, Schuman EM. A role for the cadherin family of cell adhesion molecules in hippocampal long-term potentiation. Neuron. 1998; 20:1165–1175. [PubMed: 9655504]
6. Schrick C, et al. N-cadherin regulates cytoskeletally associated IQGAP1/ERK signaling and memory formation. Neuron. 2007; 55:786–798. [PubMed: 17785185]

7. Brigidi GS, Bamji SX. Cadherin-catenin adhesion complexes at the synapse. Curr Opin Neurobiol. 2011; 21:208–214. [PubMed: 21255999]
8. Abu-Elneel K, et al. A delta-catenin signaling pathway leading to dendritic protrusions. J Biol Chem. 2008; 283:32781–32791. [PubMed: 18809680]
9. Jones SB, et al. Glutamate-induced delta-catenin redistribution and dissociation from postsynaptic receptor complexes. Neuroscience. 2002; 115:1009–1021. [PubMed: 12453475]
10. Silverman JB, et al. Synaptic anchorage of AMPA receptors by cadherins through neural plakophilin-related arm protein AMPA receptor-binding protein complexes. J Neurosci. 2007; 27:8505–8516. [PubMed: 17687028]
11. Israely I, et al. Deletion of the neuron-specific protein delta-catenin leads to severe cognitive and synaptic dysfunction. Curr Biol. 2004; 14:1657–1663. [PubMed: 15380068]
12. Matter C, Pribadi M, Liu X, Trachtenberg JT. Delta-catenin is required for the maintenance of neural structure and function in mature cortex in vivo. Neuron. 2009; 64:320–327. [PubMed: 19914181]
13. Arikkath J, et al. Delta-catenin regulates spine and synapse morphogenesis and function in hippocampal neurons during development. J Neurosci. 2009; 29:5435–5442. [PubMed: 19403811]
14. Jun G, et al. delta-Catenin Is Genetically and Biologically Associated with Cortical Cataract and Future Alzheimer-Related Structural and Functional Brain Changes. PLoS One. 2012; 7:e43728. [PubMed: 22984439]
15. Medina M, Marinescu RC, Overhauser J, Kosik KS. Hemizygosity of delta-catenin (CTNND2) is associated with severe mental retardation in cri-du-chat syndrome. Genomics. 2000; 63:157–164. [PubMed: 10673328]
16. Vrijenhoek T, et al. Recurrent CNVs disrupt three candidate genes in schizophrenia patients. Am J Hum Genet. 2008; 83:504–510. [PubMed: 18940311]
17. Kang R, et al. Neural palmitoyl-proteomics reveals dynamic synaptic palmitoylation. Nature. 2008; 456:904–909. [PubMed: 19092927]
18. Fukata Y, Fukata M. Protein palmitoylation in neuronal development and synaptic plasticity. Nat Rev Neurosci. 2010; 11:161–175. [PubMed: 20168314]
19. Noritake J, et al. Mobile DHHC palmitoylating enzyme mediates activity-sensitive synaptic targeting of PSD-95. J Cell Biol. 2009; 186:147–160. [PubMed: 19596852]
20. Keith DJ, et al. Palmitoylation of A-kinase anchoring protein 79/150 regulates dendritic endosomal targeting and synaptic plasticity mechanisms. J Neurosci. 2012; 32:7119–7136. [PubMed: 22623657]
21. Thomas GM, Hayashi T, Chiu SL, Chen CM, Huganir RL. Palmitoylation by DHHC5/8 Targets GRIP1 to Dendritic Endosomes to Regulate AMPA-R Trafficking. Neuron. 2012; 73:482–496. [PubMed: 22325201]
22. Drisdel RC, Alexander JK, Sayeed A, Green WN. Assays of protein palmitoylation. Methods. 2006; 40:127–134. [PubMed: 17012024]
23. Musleh W, Bi X, Tocco G, Yaghoubi S, Baudry M. Glycine-induced long-term potentiation is associated with structural and functional modifications of alpha-amino-3-hydroxyl-5-methyl-4-isoxazolepropionic acid receptors. Proc Natl Acad Sci U S A. 1997; 94:9451–9456. [PubMed: 9256503]
24. Lu W, et al. Activation of synaptic NMDA receptors induces membrane insertion of new AMPA receptors and LTP in cultured hippocampal neurons. Neuron. 2001; 29:243–254. [PubMed: 11182095]
25. Park M, et al. Plasticity-induced growth of dendritic spines by exocytic trafficking from recycling endosomes. Neuron. 2006; 52:817–830. [PubMed: 17145503]
26. Turrigiano GG. The self-tuning neuron: synaptic scaling of excitatory synapses. Cell. 2008; 135:422–435. [PubMed: 18984155]
27. Ren J, et al. CSS-Palm 2.0: an updated software for palmitoylation sites prediction. Protein Eng Des Sel. 2008; 21:639–644. [PubMed: 18753194]
28. Ishiyama N, et al. Dynamic and static interactions between p120 catenin and E-cadherin regulate the stability of cell-cell adhesion. Cell. 2010; 141:117–128. [PubMed: 20371349]

29. Arikkath J, et al. Erbin controls dendritic morphogenesis by regulating localization of delta-catenin. J Neurosci. 2008; 28:7047–7056. [PubMed: 18614673]
30. Restituito S, et al. Synaptic autoregulation by metalloproteases and gamma-secretase. J Neurosci. 2011; 31:12083–12093. [PubMed: 21865451]
31. El Sayegh TY, et al. Phosphorylation of N-cadherin-associated cortactin by Fer kinase regulates N-cadherin mobility and intercellular adhesion strength. Mol Biol Cell. 2005; 16:5514–5527. [PubMed: 16176974]
32. Saglietti L, et al. Extracellular interactions between GluR2 and N-cadherin in spine regulation. Neuron. 2007; 54:461–477. [PubMed: 17481398]
33. Murakoshi H, Wang H, Yasuda R. Local, persistent activation of Rho GTPases during plasticity of single dendritic spines. Nature. 2011; 472:100–104. [PubMed: 21423166]
34. Kim H, et al. Delta-catenin-induced dendritic morphogenesis. An essential role of p190RhoGEF interaction through Akt1-mediated phosphorylation. J Biol Chem. 2008; 283:977–987. [PubMed: 17993462]
35. Ochiishi T, Futai K, Okamoto K, Kameyama K, Kosik KS. Regulation of AMPA receptor trafficking by delta-catenin. Mol Cell Neurosci. 2008; 39:499–507. [PubMed: 18602475]
36. Park M, Penick EC, Edwards JG, Kauer JA, Ehlers MD. Recycling endosomes supply AMPA receptors for LTP. Science. 2004; 305:1972–1975. [PubMed: 15448273]
37. Kennedy MJ, Davison IG, Robinson CG, Ehlers MD. Syntaxin-4 defines a domain for activity-dependent exocytosis in dendritic spines. Cell. 2010; 141:524–535. [PubMed: 20434989]
38. Ohno Y, et al. Analysis of substrate specificity of human DHHC protein acyltransferases using a yeast expression system. Mol Biol Cell. 2012; 23:4543–4551. [PubMed: 23034182]
39. Nanes BA, et al. p120-catenin binding masks an endocytic signal conserved in classical cadherins. J Cell Biol. 2012; 199:365–380. [PubMed: 23071156]
40. Huber AH, Weis WI. The structure of the beta-catenin/E-cadherin complex and the molecular basis of diverse ligand recognition by beta-catenin. Cell. 2001; 105:391–402. [PubMed: 11348595]
41. Abe K, Chisaka O, Van Roy F, Takeichi M. Stability of dendritic spines and synaptic contacts is controlled by alpha N-catenin. Nat Neurosci. 2004; 7:357–363. [PubMed: 15034585]
42. Martinez MC, Ochiishi T, Majewski M, Kosik KS. Dual regulation of neuronal morphogenesis by a delta-catenin-cortactin complex and Rho. J Cell Biol. 2003; 162:99–111. [PubMed: 12835311]
43. Fukata Y, et al. Local palmitoylation cycles define activity-regulated postsynaptic subdomains. J Cell Biol. 2013; 202:145–161. [PubMed: 23836932]
44. Misra C, et al. Regulation of synaptic structure and function by palmitoylated AMPA receptor binding protein. Mol Cell Neurosci. 2010; 43:341–352. [PubMed: 20083202]
45. Nuriya M, Huganir RL. Regulation of AMPA receptor trafficking by N-cadherin. Journal of neurochemistry. 2006; 97:652–661. [PubMed: 16515543]
46. Maguschak KA, Ressler KJ. Beta-catenin is required for memory consolidation. Nat Neurosci. 2008; 11:1319–1326. [PubMed: 18820693]
47. Radulovic J, Kammermeier J, Spiess J. Relationship between fos production and classical fear conditioning: effects of novelty, latent inhibition, and unconditioned stimulus preexposure. J Neurosci. 1998; 18:7452–7461. [PubMed: 9736664]
48. Xie C, Markesbery WR, Lovell MA. Survival of hippocampal and cortical neurons in a mixture of MEM+ and B27-supplemented neurobasal medium. Free Radic Biol Med. 2000; 28:665–672. [PubMed: 10754261]
49. Durocher Y, Perret S, Kamen A. High-level and high-throughput recombinant protein production by transient transfection of suspension-growing human 293-EBNA1 cells. Nucleic Acids Res. 2002; 30:E9. [PubMed: 11788735]
50. Sun Y, Bamji SX. beta-Pix modulates actin-mediated recruitment of synaptic vesicles to synapses. J Neurosci. 2011; 31:17123–17133. [PubMed: 22114281]
51. Diering GH, Mills F, Bamji SX, Numata M. Regulation of dendritic spine growth through activity-dependent recruitment of the brain-enriched Na(+)/H(+) exchanger NHE5. Mol Biol Cell. 2011; 22:2246–2257. [PubMed: 21551074]

52. Huang K, et al. Neuronal palmitoyl acyl transferases exhibit distinct substrate specificity. FASEB J. 2009; 23:2605–2615. [PubMed: 19299482]

53. Brigidi GS, Bamji SX. Detection of Protein Palmitoylation in Cultured Hippocampal Neurons by Immunoprecipitation and Acyl-Biotin Exchange (ABE). J Vis Exp. 2013

54. Milnerwood AJ, et al. Memory and synaptic deficits in Hip14/DHHC17 knockout mice. Proc Natl Acad Sci U S A. 2013; 110:20296–20301. [PubMed: 24277827]

55. Tapia L, et al. Progranulin deficiency decreases gross neural connectivity but enhances transmission at individual synapses. J Neurosci. 2011; 31:11126–11132. [PubMed: 21813674]

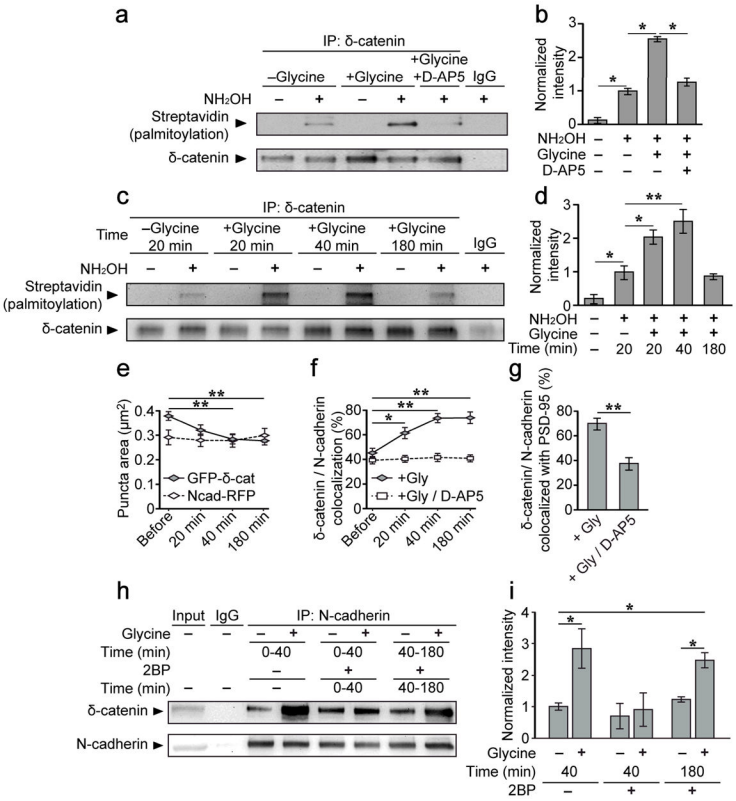

Figure 1. δ-catenin palmitoylation and its association with synaptic N-cadherin is increased following activity

(**a–d**) ABE chemistry and western blotting for streptavidin-HRP was used to determine palmitoylation of immunoprecipitated proteins. Omission of NH_2OH controlled for non-specific incorporation of biotin. (**a**, **b**) δ-catenin palmitoylation increased 40 min after glycine treatment but not glycine+D-AP5 (50μM; n=4, p=0.017, $F_{2,9}$=6.59). (**c**, **d**) δ-catenin palmitoylation peaked at 40 mins and returned to baseline 180 mins after glycine treatment (n=4, p=0.001, $F_{4,10}$=19.01). (**e–g**) 14 DIV hippocampal neurons transfected with GFP-δ-catenin and N-cadherin-RFP were imaged immediately before and 20, 40 and 180 min after glycine treatment, and stained for PSD-95 *post hoc*. (**e**) Glycine treatment decreased the area of GFP-δ-catenin (GFP-δ-catenin: n=19, p<0.001, $F_{3,18}$=10.26; N-cadherin-RFP: n=19, p=0.476, $F_{3,18}$=21.69), (**f**) increased δ-catenin/N-cadherin colocalization (Glycine: n=19, p<0.001, $F_{3,18}$=4.171; Glycine+D-AP5: n=9, p=0.755, $F_{3,8}$=0.399) and (**g**) increased the colocalization of δ-catenin/N-cadherin with PSD-95, compared to cells treated with glycine +D-AP5 (n=19, 9, p=0.001, student's t-test). (**h, i**) δ-catenin/N-cadherin interactions were enhanced 40 min following glycine treatment, and abolished when 2-bromopalmitate (2BP, 50μM) was applied from 0 to 40 min, but not from 40–180 min, after stimulation (n=7, p=0.007, $F_{5,24}$=4.15). n values indicate (**b**, **d**, **i**) the number of separate blots from separate cell cultures, or (**e–g**) the number of cells from 3 separate cultures. Graphs show mean ± SEM. (**b**, **d**, **i**) ***p<0.05, ****p<0.01; one-way ANOVA; Tukey's test *post hoc*. (**e, f**) ***p<0.05, ****p<0.01; repeated measures one-way ANOVA, Tukey's test *post hoc*; (**g**) ****p<0.01; student's t-test. Full length blots from (**a**, **c**, **h**) are presented in Supplementary Figure 6.

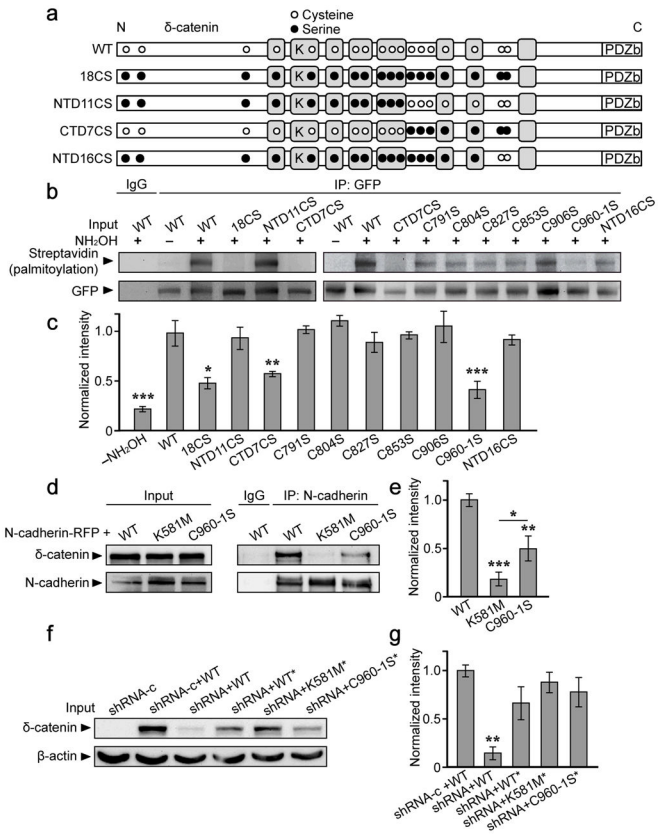

Figure 2. Palmitoylation of δ-catenin occurs at cysteines 960 and 961, and requires lysine 581 for binding to N-cadherin

(**a**) Schematic depiction of δ-catenin constructs, N-terminally tagged with GFP (not shown), and illustrating the approximate localization of all 18 cysteine residues (white circles), as well as cysteine to serine mutations (black circles). Lysine 581 (K) is located within the third Armadillo repeat domain (grey boxes), and the PDZ-binding motif (PDZb) at the C-terminus. (**b**, **c**) GFP-δ-catenin constructs were transfected into HEK293T cells for 36–48 hrs and lysates immunoprecipitated with anti-GFP. Following ABE labeling, blots were probed with anti-streptavidin to determine palmitoylation of the specified δ-catenin construct. (n=3–5 blots from separate cultures, $p<0.001$, $F_{11,41}=10.18$). (**d**, **e**) HEK293T cells were transfected with the indicated GFP-tagged δ-catenin constructs plus N-cadherin-RFP, and lysates immunoprecipitated with anti-N-cadherin. (n=3, $p<0.001$, $F_{2,6}=32.87$). (**f**, **g**) 293T cells were transfected with a control shRNA (shRNA-c) or δ-catenin shRNA, plus the indicated GFP-δ-catenin constructs (*denotes shRNA-resistance) (n=4, $p=0.005$, $F_{4,13}=6.41$). The n value indicates the number of separate blots from separate cell cultures. *****$p<0.05$, ******$p<0.01$, *******$p<0.001$; one-way ANOVA, Tukey's test *post hoc*. Full length blots from (**b**, **d**, **f**) are presented in Supplementary Figure 6.

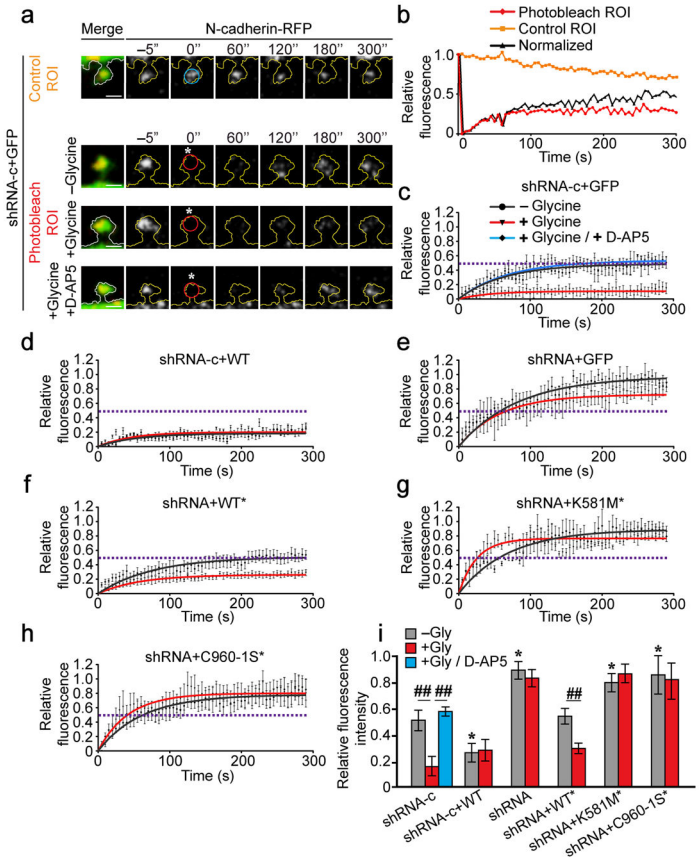

Figure 3. δ-catenin palmitoylation is required for activity-induced stabilization of N-cadherin within dendritic spine heads

(**a**) Cells were photobleached at 0 s (”; white asterisk) within a 1μm diameter ROI. Fluorescence within a photobleached ROI (red circle) was normalized to non-photobleached ROI in adjacent spines (blue circle). Scale bar=1μm. (**b**) Fluorescence recovery within photobleached and non-photobleached ROIs (from top two panels in **a**) and the normalization for bleaching. (**c–h**) Normalized fluorescence recovery of N-cadherin-RFP. Dashed lines represent the plateau for fluorescence recovery in control cells (**c**). Points with error bars represent mean ± SEM, solid lines represent single exponential fit. Statistical tests compare plateau values from exponential fits ± SEM. Neurons were obtained from ≥ 3 separate cultures. (**c**) n=10 cells, −glycine; 15 cells, +glycine; n=5 cells, glycine+D-AP5; p=0.003, $F_{2,27}$=7.15, one-way ANOVA. (**d**) n=11 cells, –glycine; 5 cells, +glycine; p=0.991; student’s t-test. (**e**) n=18 cells, −glycine; 8 cells, +glycine; p=0.099, student’s t-test). (**f**) n=18 cells, −glycine; 9 cells, +glycine; p=0.003, student’s t-test. (**g**) n=12 cells, −glycine; 9 cells, +glycine; p=0.223, student’s t-test. (**h**) n=25 cells, −glycine; 8 cells, +glycine; p=0.92, t-test. (**i**) The mobile fraction of N-cadherin-RFP (fluorescence within the ROI at the 5 min time point, normalized for photobleaching; mean ± SEM; p<0.001, $F_{12,140}$=8.03; one-way ANOVA). *****p<0.05, one-way ANOVA, Tukey’s test *post hoc*, relative to control cells expressing shRNA-c, in the absence of glycine; ##p<0.01, Tukey’s test *post hoc*, relative to same transfection condition in the absence of glycine.

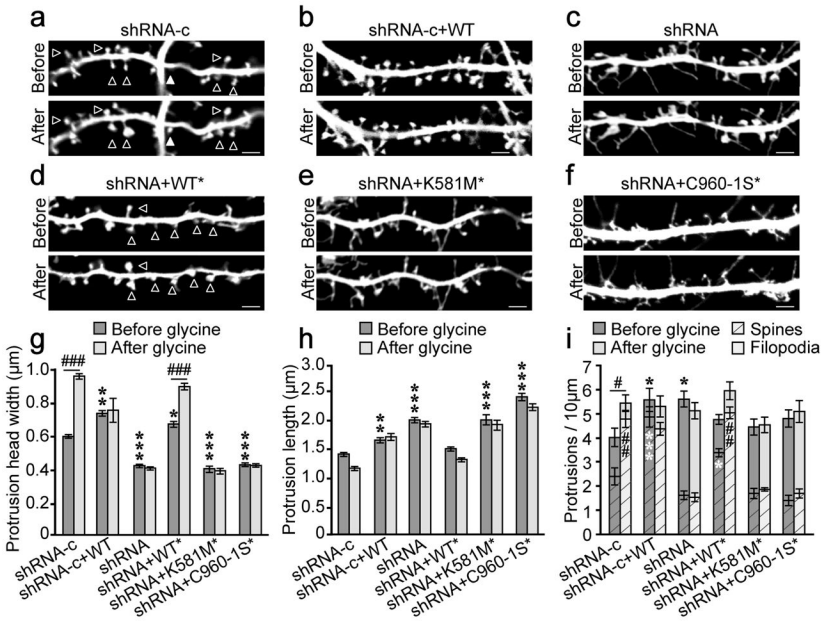

Figure 4. δ-catenin palmitoylation is required for activity-induced spine remodeling

Primary dendrites were imaged before and again 40–60 min after glycine treatment. (**a**) n=12 cells, 803 spines; (**b**) n=7 cells, 396 spines; (**c**) n=10 cells, 529 spines, (**d**) n=10 cells, 606 spines; (**e**) n=8 cells, 352 spines; (**f**) n=10 cells, 535 spines. Scale bar=2µm. (**g**) Protrusion head width before and after glycine treatment ($p<0.001$, $F_{5,6430}=127.57$ [between groups effect]; $p<0.001$, $F_{1,6430}=43.13$ [glycine treatment effect]). (**h**) Length of protrusions before and after glycine treatment ($p<0.001$, $F_{5,6430}=213.45$ [between groups effect]; $p<0.001$, $F_{1,6430}=11.57$ [glycine treatment effect]. (**i**) The density of total protrusions (mean represented by crosshatched bars plus solid bars; top error bars represent total protrusion SEM; $p=0.005$, $F_{5,102}=2.23$ [between groups effect]; $p=0.04$, $F_{1,102}=4.32$ [glycine treatment effect]; two-way ANOVA), filopodia (solid bars), and spines (crosshatched bars ± SEM; $p<0.001$, $F_{5,102}=65.05$ [between groups effect]; $p<0.001$, $F_{5,102}=18.71$ [glycine treatment effect]; two-way ANOVA) before and after glycine treatment. Cells were obtained from ≥3 separate cultures. Graphs represent mean ± SEM. (**g**, **h**) ***p<0.05, ****p<0.01, *****p<0.001; two-way ANOVA, Bonferonni's test *post hoc*, relative to shRNA-c before glycine treatment. ###p<0.001; Bonferonni's test *post hoc*, relative to same condition before glycine. (**i**) ***(black) above bars compare total protrusions relative to shRNA-c cells before glycine, ***(white) within crosshatched bars compare spines relative to shRNA-c before glycine; # above bars compare total protrusions within groups before and after glycine, # within crosshatched bars compare spines within groups before and after glycine. #/***p<0.05, ##/****p<0.01, *****p<0.001 two-way ANOVA, Bonferonni's test post-hoc.

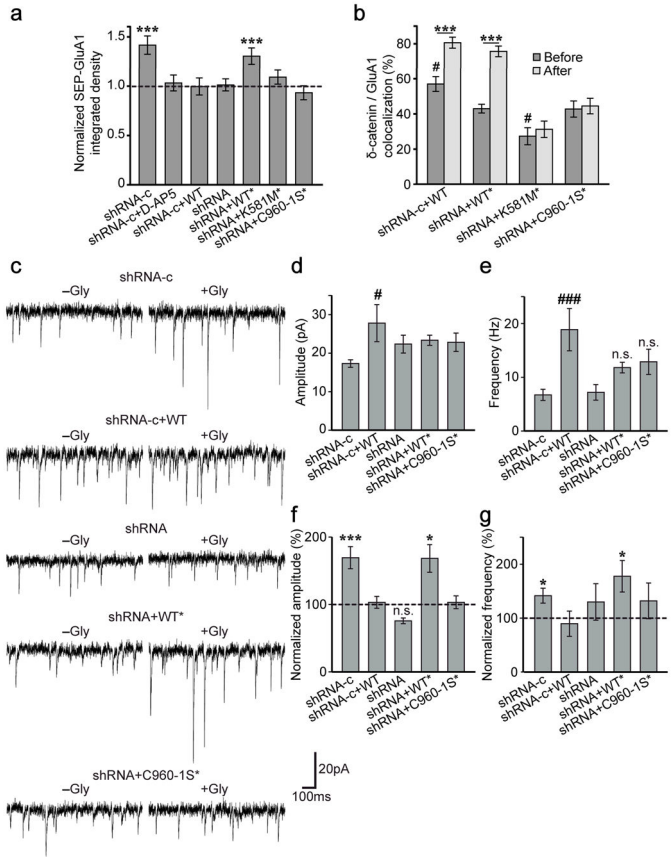

Figure 5. δ-catenin palmitoylation is required for activity-induced AMPA receptor insertion and changes in mEPSCs

(**a**, **b**) Cells were imaged before and 40–60 min after indicated treatments. (**a**) Integrated density (IntDen) of pre-existing SEP-GluA1 puncta normalized to the same puncta before treatment (dashed line). Cell number and p values from paired t-tests: shRNA-c (n=22, p<0.001), shRNA-c+D-AP5 (n=9, p=0.91), shRNA-c+WT (n=9, p=0.865), shRNA (n=10, p=0.942), shRNA+WT* (n=14, p<0.001), shRNA+K581M* (n=13, p=0.133), and shRNA +C960-1S* (n=9, p=0.176). (**b**) Percent δ-catenin/GluA1 colocalization (p<0.001, $F_{3,49}$=8.25; one-way ANOVA). Crosshatches denote significance among “before” groups relative to shRNA+WT*, asterisks denote significance within groups before and after glycine: shRNA-c+WT (n=12, p<0.001), shRNA+WT* (n=15, p<0.001), shRNA+K581M* (n=12, p=0.552), and shRNA+C960-1S* (n=14, p=0.494). (**c–g**) Whole-cell recordings (held at −65mV) 40 min after indicated treatments. (**c**) Representative mEPSC traces. (**d**) Basal mEPSC amplitude increased in shRNA-c+WT cells (p=0.031, $F_{4,45}$=2.928, one-way ANOVA). (**e**) Basal mEPSC frequency was increased in shRNA-c+WT cells (p<0.001, $F_{4,45}$=6.056; one-way ANOVA). (**f**, **g**) Percent mEPSC amplitude and frequency 40 min after glycine, normalized to the mean in untreated cells (dashed line). n values in −glycine or +glycine groups, and p values from student’s t-tests for amplitude and frequency, respectively: shRNA-c (n=17, 23; p<0.001; p=0.048), shRNA-c+WT* (n=9, 8; p=0.857; p=0.741), shRNA (n=9, 7, p=0.076; p=0.440), shRNA+WT* (n=7, 10; p=0.016; p=0.048), shRNA+960-1S* (n=8, 7; p=0.801; p=0.209). Graphs represent mean ± SEM. (**a**, **b**)

*****p<0.05, ******p<0.01, *******p<0.001; paired t-test. #p<0.05, one-way ANOVA with Tukey's test *post hoc*. (**d–g**) #p<0.05, ###p<0.001; one-way ANOVA, Tukey's test *post hoc*. *****p<0.05, *******p<0.001; student's t-test.

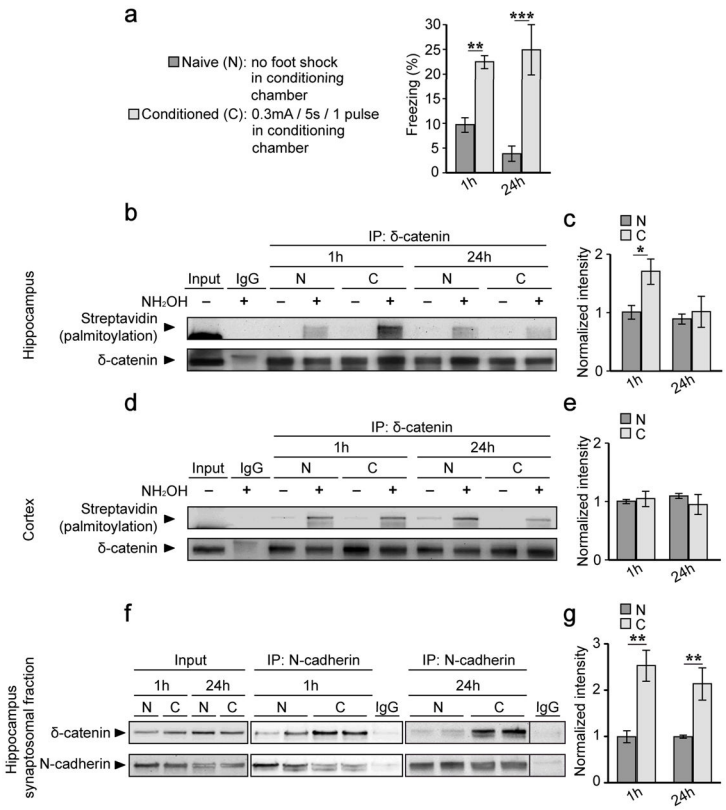

Figure 6. Context-dependent fear conditioning increases δ-catenin palmitoylation and N-cadherin associations in the hippocampus

(**a**) 6–9 week old male mice exhibited increased freezing 1 hour (h) and 24 h following contextual fear conditioning (conditioned group, C) compared to mice which did not receive a foot shock (Naïve group, N) (n=10 mice per group, per timepoint; $p<0.001$, $F_{1,36}=35.89$ [treatment effect]; $p=0.539$, $F_{1,36}=0.38$ [timepoint effect]). Hippocampal (**b**, **c**) or cortical (**d**, **e**) lysates from naïve and conditioned mice were immunoprecipitated with anti-δ-catenin or IgG, and and palmitoylation levels determined using ABE chemistry. (**b**, **c**) Palmitoylation of δ-catenin is transiently increased in the hippocampus of conditioned mice (n=5 blots from 5 separate animals; $p=0.034$, $F_{1,16}=5.37$ [treatment effect]; $p=0.037$, $F_{1,16}=5.17$[timepoint effect]). (**d**, **e**) Palmitoylation levels of δ-catenin are similar in the cortex of naïve and conditioned mice (n=3 blots from 3 separate animals; $p=0.463$, $F_{1,8}=0.59$ [treatment effect]; $p=0.978$, $F_{1,8}=0.1$ [timepoint effect]). (**f**, **g**) P2 synaptosomes from hippocampal lysates were isolated and immunoprecipitated with anti-N-cadherin. There is an increase in δ-catenin bound to N-cadherin in the hippocampus of conditioned mice 1 h and 24 h after training. The IgG lane in the blot on the right was cropped from another position within the same blot. (n=3 and 5 blots from 3 and 5 separate animals 1 h, and 24 h post-training, respectively; $p<0.001$, $F_{1,12}=24.95$ [treatment effect]; $p=0.492$, $F_{1,12}=0.50$ [timepoint effect]). All graphs represent mean ± SEM. *****$p<0.05$, ******$p<0.01$, *******$p<0.001$, two-way ANOVA, Bonferroni's test *post hoc*. Full length blots of those shown in (**b**, **d**, **f**) are presented in Supplementary Figure 6.

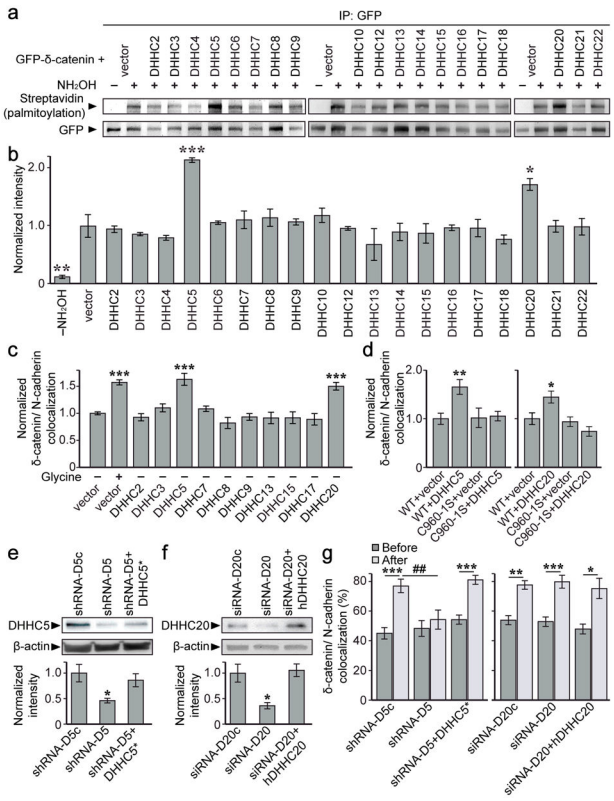

Figure 7. DHHC5 and 20 palmitoylate δ-catenin but activity-induced recruitment of δ-catenin to N-cadherin is mediated by DHHC5

(**a**, **b**) Palmitoylation of GFP-δ-catenin co-transfected with the indicated DHHC constructs in HEK293T cells (n=3–6 blots from separate cultures, $p<0.001$, $F_{19,36}=7.154$). (**c**) Colocalization of GFP-δ-catenin and N-cadherin-RFP in cells expressing the indicated DHHCs ($p<0.001$, $F_{11,834}=15.4$). Cell number from 3–10 cultures: vector –glycine (n=262), vector +glycine (n=200), DHHC2 (n=35), DHHC3 (n=47), DHHC5 (n=39), DHHC7 (n=31), DHHC8 (n=56), DHHC9 (n=49), DHHC13 (n=22), DHHC15 (n=18), DHHC17 (n=24), DHHC20 (n=63). (**d**) δ-catenin palmitoylation is essential for DHHC5 ($p=0.004$, $F_{3,75}=4.67$) and DHHC20-induced ($p=0.005$, $F_{3,86}=6.559$) clustering of δ-catenin/N-cadherin. Number of cells from 3 cultures: WT+vector (DHHC5 experiment; n=22), WT +DHHC5 (n=17), C960-1S+vector (n=20), C960-1S+DHHC5 (n=20), WT+vector (DHHC20 experiment; n=23), WT+DHHC20 (n=20), C960-1S+vector (n=12), C960-1S +DHHC20 (n=20). (**e**, **f**) RNAi-mediated knockdown of DHHC5 and DHHC20 in 6DIV hippocampal neurons. (**e**) n=5 blots from 5 cultures, $p=0.022$, $F_{2,12}=5.29$ (*denotes shRNA-resistance). (**f**) n=3 blots from 3 cultures, $p=0.019$, $F_{2,6}=8.29$ (hDHHC20 denotes human DHHC20). (**g**) Knockdown of DHHC5, but not DHHC20 abolished activity-induced increases in GFP-δ-catenin/N-cadherin-RFP colocalization. Cell number and p values from paired t-tests before/after activity: DHHC5 ($p<0.001$, $F_{5,78}=5.29$, one-way ANOVA); shRNA-D5c (n=15, $p<0.001$), shRNA-D5 (n=13, $p=0.288$), shRNA-D5+DHHC5* (n=14, $p<0.001$). DHHC20: ($p<0.001$, $F_{5,66}=13.65$, one-way ANOVA); siRNA-D20c (n=11, $p=0.004$), siRNA-D20 (n=13, $p<0.001$), siRNA-D20+hDHHC20 (n=12, $p=0.012$). Graphs represent mean ± SEM. (**b–f**) ***p<0.05, ****p<0.01, *****p<0.001, one-way ANOVA with

Tukey's test *post hoc*. (**g**) ***p<0.05, ****p<0.01, *****p<0.001, paired t-test; ##p<0.01, one-way ANOVA with Tukey's test *post hoc*. Full length blots from (**a**, **e**, **f**) shown in Supplementary Figure 6.

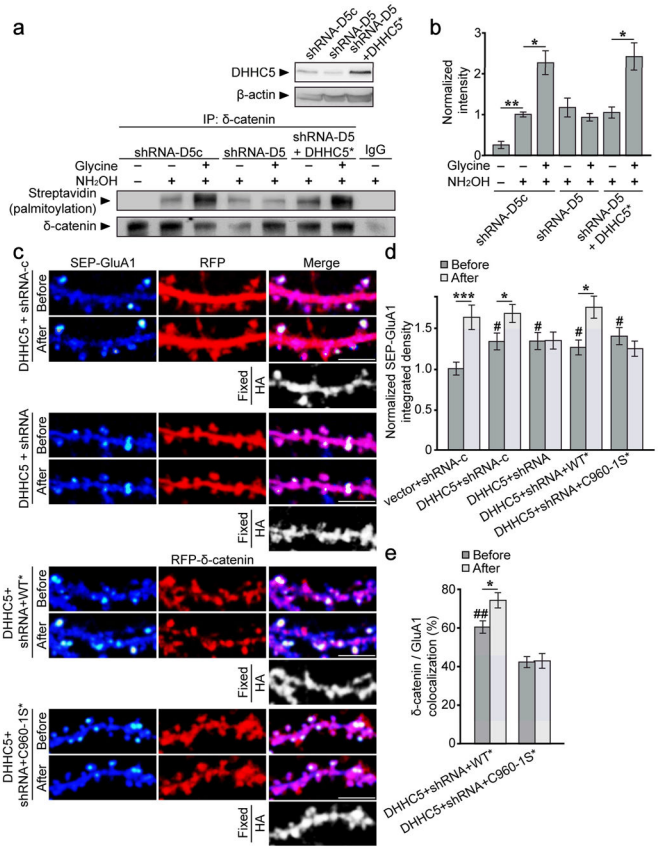

Figure 8. DHHC5 is required for activity-induced palmitoylation of δ-catenin and surface AMPAR insertion

(**a** *top*) shRNA-D5 reduced DHHC5 levels at 12 DIV (shRNA-D5c[1.0 ± 0.13]: shRNA-D5 [0.62 ± 0.042], shRNA-D5+DHHC5* [0.89 ± 0.044]; one-way ANOVA, p=0.042, $F_{2,6}$=5.57). (**a** *bottom*, **b**) Knockdown of DHHC5 abolishes activity-induced palmitoylation of δ-catenin (n=3 blots from 3 separate cultures, p=0.002, $F_{6,14}$=10.03). (**c**) Confocal images of hippocampal neurons transfected with the indicated constructs before and 40–60 min after glycine treatment. SEP-fluorescent puncta are pseudocolored in heat maps. DHHC5-HA overexpression was confirmed by *post hoc* immunostaining for HA. Scale bar=5μm. (**d**) IntDen of SEP-GluA1 puncta, normalized to the same puncta before glycine treatment. n values indicate cell number from ≥3 separate cultures, and p values from paired t-tests: vector+shRNA-c (14, p<0.001), DHHC5+δ-catenin shRNA-c (15, p=0.006), DHHC5+δ-catenin shRNA (13, p=0.857), DHHC5+δ-catenin shRNA+δ-catenin WT* (16, p=0.002), and DHHC5+δ-catenin shRNA+δ-catenin C960-1S* (13, p=0.161). DHHC5 overexpression increased basal SEP-GluA1 IntDen (one-way ANOVA; p=0.001, $F_{9,132}$=4.141). Crosshatches denote significance among “before” groups relative to vector+shRNA-c, asterisks denote significance within groups before and after glycine. (**e**) Colocalization of indicated δ-catenin constructs with GluA1 (one-way ANOVA; p<0.001, $F_{3,54}$=19.29). Crosshatches denote significance among “before” groups relative to DHHC5+shRNA +C960-1S*. WT*/GluA1 colocalization increased following activity (paired t-test; p=0.005), whereas C960-1S*/GluA1 colocalization did not (paired t-test; p=0.741). Graphs represent mean ± SEM. (**b**) *p<0.05, one-way ANOVA with Tukey’s test *post hoc*. (**d, e**) *p<0.05,

*******p<0.001, paired t-test; #p<0.05, ##p<0.01, one-way ANOVA with Tukey's test *post hoc.* Full-length blots from (**a**) are presented in Supplementary Figure 6.